ELSEVIER

Journal of Nuclear Materials 279 (2000) 344–350

journal of nuclear materials

www.elsevier.nl/locate/jnucmat

Residual carbon impurities in Zr–2.5Nb and their effect on deuterium pickup

Robert A. Ploc

Atomic Energy of Canada Limited, Fuel Channel Components Branch, Chalk River, Ont., Canada K0J 1J0

Received 7 May 1999; accepted 5 November 1999

Abstract

The presence of residual carbon in Zr–2.5Nb at parts per million (ppm) levels affects the alloy's rates of oxide film growth and deuterium absorption (in 573 K lithiated heavy-water). Pickup rates increase with increasing carbon concentrations between 40 and 300 ppm with a possible inflection in the kinetic curves in the vicinity of 120 ppm. Increased rates are likely due to enhanced development of an inter-connected, large-scale, pore network within the oxide film. Oxides on Zr–2.5Nb containing 145 ppm carbon appear to be fully stoichiometric with a well developed network of large pores, while the oxide on the 85 ppm C alloy contains a high density of fine pores and is likely sub-stoichiometric.

1. Introduction

Most nuclear power reactors operate in pressurized aqueous environments with temperatures in excess of 525 K. Under these conditions, zirconium alloy reactor components corrode and absorb hydrogen. In light-water (H_2O) cooled reactors, core materials are usually Zircaloy [1] while in the Canadian CANDU [2] system, moderated and cooled with heavy-water (D_2O), the pressure-containing components (pressure tubes) are manufactured from Zr–2.5Nb. While Zircaloy and Zr–2.5Nb are both dilute alloys of zirconium, there are large differences in the amounts of hydrogen they absorb. Typically the Zircaloys absorb 30–100% of the hydrogen generated by the corrosion process (percent theoretical pickup) and Zr–2.5Nb absorbs less than 10%. The presence of Nb in Zirconium obviously plays an instrumental role in limiting hydrogen pickup. The solubility of hydrogen at 575 K is approximately 60 ppm at which point brittle hydrides form, which can compromise the integrity of a pressure containing component.

Although hydrogen absorption rates in the CANDU environment are low, steps to minimize absorption are required because the design lifetime of a pressure tube is approximately 30 yr. Varying the concentration of the primary alloying elements in Zircaloy results in significant differences in the pickup rate of hydrogen. Although this effect is likely due to the second phase precipitate size and distribution, it is also known that the purer the zirconium, the lower the hydrogen ingress rate [1]. Impurities, in general, accelerate pickup.

Impurity limits in Zr–2.5Nb are normally set as low as practical without compromising the economical viability of the alloy. In terms of deuterium ingress, the benefit or liability of a specific impurity is rarely known, especially when it is in the ppm range of concentration. Understanding and controlling the behaviour of an impurity could extend component lifetimes and increase safety margins. Residual carbon is a case in point; carbon being detrimental at concentrations greater than 0.5% [2,3], but its effect in the ppm range is unknown.

It is difficult to elucidate the role of a specific impurity because of synergism with other elements. For instance, iron or silicon can be present as carbides or in solid solution depending on the material fabrication history. The behaviour of carbon as a precipitate is

[1] Zircaloy-2: 1.2–1.7% Sn, 0.07–0.2% Fe, 0.05–0.15% Cr, 0.03–0.08% Ni. Zircaloy-4: 1.2–1.7% Sn, 0.18–0.24% Fe, 0.07–0.13% Cr, Ni-free.

[2] CaNadian Deuterium Uranium, registered Trade Mark of Atomic Energy of Canada Limited.

0022-3115/00/$ - see front matter
PII: S0022-3115(99)00282-2

likely to be different than when it is in solid solution. Therefore, merit testing of modified alloys must use a consistent base material for alloy fabrication to ensure an invariant impurity profile (except for the element being tested). As pure a material as possible should be used to prevent data distortion arising from an unsuspected dominate impurity.

A generally accepted mechanism for hydrogen (deuterium) ingress into zirconium alloys has not yet been proposed. Measurements of hydrogen profiles [4], nuclear activation studies [5] and examination of oxide structures [6,7] have all been to little avail. However, an important observation that has come from these studies is that zirconia films are porous (mercury porosimetry [8,9], electrochemical impedance analysis [10] and electron microscopy of oxide cross-sections [11]). Porosity greatly increases the oxide surface area on which water molecules can be reduced and proton absorption (or recombination) can transpire. As well, inter-connected porosity gives access of the corroding medium to the oxide/metal interface.

This report describes the phenomenological role of carbon, as an impurity, its affect on deuterium pickup and how carbon likely modifies the oxide microstructure.

2. Experimental materials

Coupons of Zr–2.5Nb were corroded at 573 K (300°C) in autoclaves containing pD 10.5 (RT, Li_2O additions) heavy-water (D_2O). The corrosion coupons were taken from two sources:

1. Zr–2.5Nb–xC (40 ppm $\leqslant x \leqslant$ 300 ppm by weight) drop-castings (DC), and
2. CANDU pressure tubes (PT).

Each batch of PT specimens, cut from each of several PTs, are associated with a unique impurity profile and a unique manufacturing schedule. As well, the base zirconium used in the manufacturing of each PT would have come from one of three international suppliers: USA, France or Russia. The DCs, on the other hand, were all manufactured by the same supplier and from the same zirconium stock which, except for tungsten, ensured an invariant impurity profile. Tungsten contamination arose from the 'non-consumable' electrode used in melting. Table 1 lists the concentrations of four impurities (and oxygen) for the specimens used in this report.

PT and DC specimens have different metal grain structures. PT extrusion results in the metal grains being flattened radially and elongated longitudinally. Looking along the longitudinal axis of the pressure tube, the grain aspect ratio can be seen to be about 10/1 while looking in the transverse direction the ratio is more like 40/1 or 50/1. Alloy strips produced from the DCs were cross-rolled to approximate the PT grain morphology but the resultant aspect ratios were considerably less pronounced than those of the PTs.

PT surfaces were prepared for corrosion by grinding with SiC to a 320-grit finish. DCs were machined finished to RMS 40 and burrs removed using 320-grit SiC. All specimens were degreased for 10 min in caustic soda (50%, by weight) at 323–333 K (50–60°C) followed by dipping in room temperature distilled water and finally washed in stirred distilled water for 1 h at 323–333 K. Specimens were dried on filter paper.

For each weight datum, a microbalance was used to obtain four non-consecutive weighings per specimen. The highest and lowest weights were discarded and the remaining two were averaged. Deuterium absorption was measured using Hot Vacuum Extraction (1375 K) Mass Spectrograph (HVEMS). Overall accuracy and precision was 5%.

3. Results and discussion

3.1. Kinetics

Fig. 1 shows deuterium and oxygen pickup as a function of days of corrosion (exposure) and carbon

Table 1
Impurities in pressure tube off-cuts (F) and drop-castings (D) in weight (first line) and atomic ppm (second line)

	$F1$	$F2$	$F3$	$F4$	$F5$	$D1$	$D2$	$D3$	$D4$	$D5$	$D6$	$D7$	$D8$
C	85	95	110	130	145	45	80	100	125	150	170	210	300
	645	721	835	986	1100	342	608	759	949	1025	1290	1539	2275
Fe	420	365	460	830	430	190	180	185	185	185	185	180	185
	686	596	751	1357	720	310	294	302	302	302	302	294	302
Si	25	25	30	75	60	–	–	–	–	–	–	–	–
	81	81	97	244	195	–	–	–	–	–	–	–	–
W	<25	<25	<25	<25	<25	30	<30	<30	55	300	80	85	220
	<12	<12	<12	<12	<12	15	<15	<15	27	149	40	42	109
O	1100	1200	1140	1100	1130	550	510	510	540	520	510	520	510

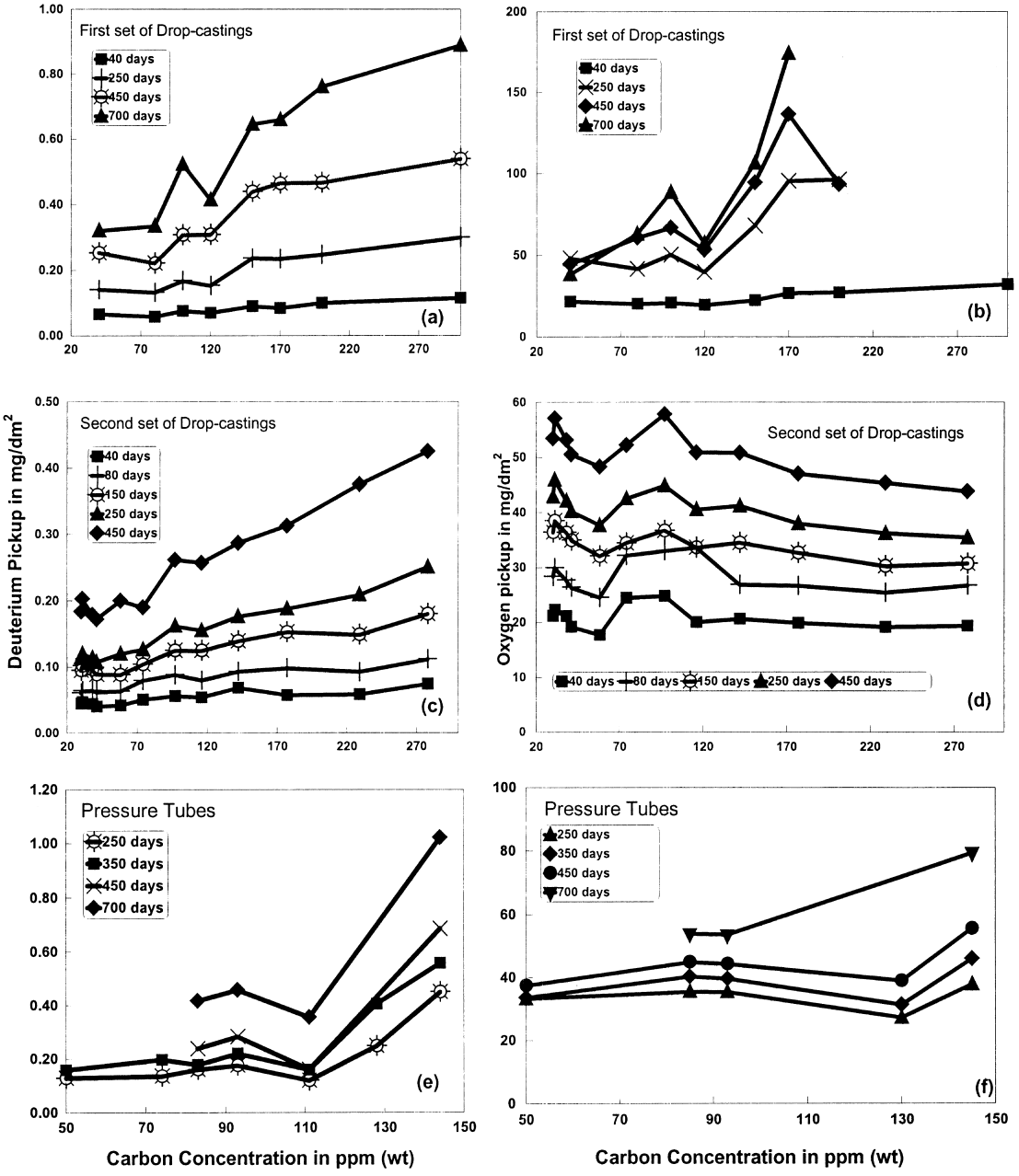

Fig. 1. Oxygen (graphs on right) and deuterium (graphs on left) pickup in mg/dm^2 as a function of residual carbon concentration and days of corrosion. Pressure tube data were available for a limited carbon concentration range only. (a)/(b), (c)/(d) and (e)/(f) correspond to the first and second sets of drop-castings and pressure tubes, respectively.

concentration for two DC (Figs. 1(a)–(d)) and one PT series (Figs. 1(e) and (f)). Except for Fig. 1(d), both oxygen and deuterium pickup increase with increasing carbon concentration, the trend becoming more pronounced with increasing exposure.

In Fig. 1(e), the suppressed deuterium pickup at 110 ppm carbon likely represents a change in the corrosion mechanism (see also Fig. 1(f) for 700 days). Though the inflection was also seen in the data from the first set of DCs for exposures of less than 250 days, it was never observed in the second DC set. Plots of the percent theoretical pickup (the percentage of the corrosion generated deuterium that is absorbed by the specimen) as a function of time for the DCs produced relatively flat

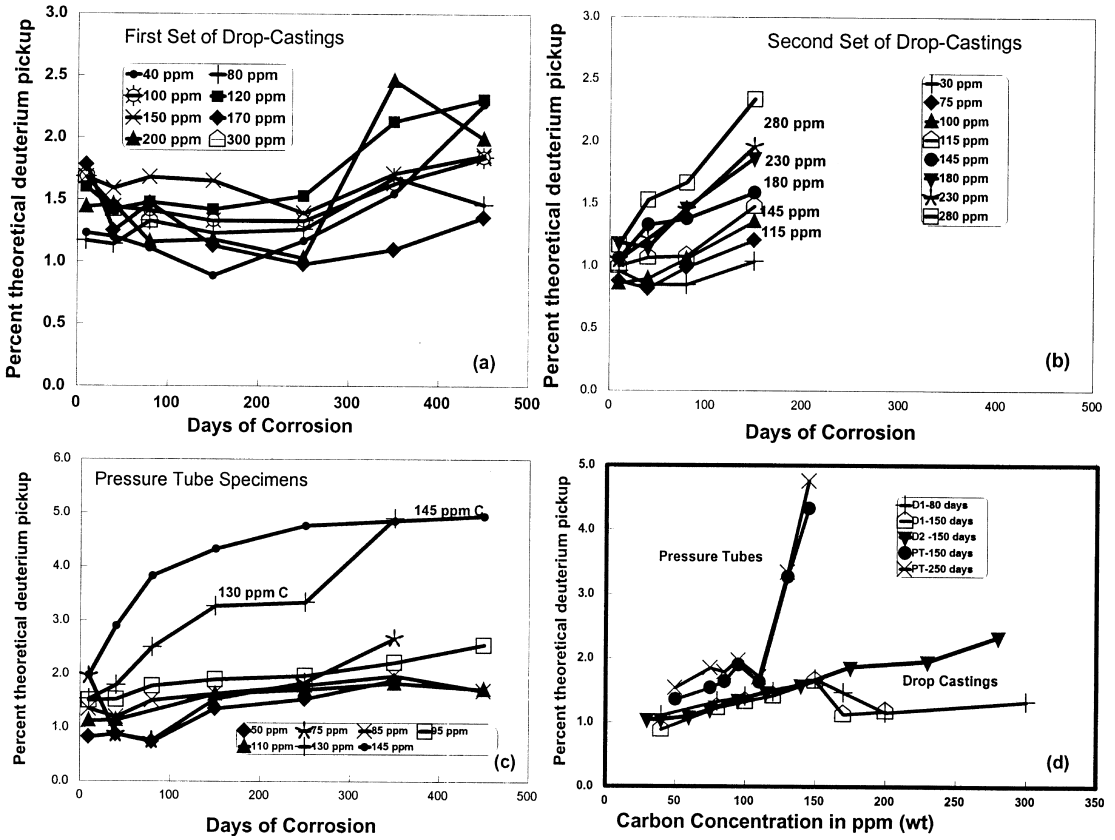

Fig. 2. Percent theoretical pickup of the deuterium generated during the corrosion reaction. (a) and (b) are for the two sets of drop-castings, (b) is truncated due to the lack of data. Sudden increases in the percent theoretical pickup, as in (a), are usually artifacts due to oxide spalling. (c) and (d) are for the Pressure Tube specimens, (c) as a function of time and (d) as a function of carbon concentration.

curves. On the other hand, the same plots for the PTs indicated a change in corrosion mechanism for carbon values above 110 ppm. Figs. 2(a) and (b) are for the two sets of drop castings while (c) is for the pressure tubes. In Fig. 2(c), the curves have a characteristically different shape above 110 ppm carbon, indicating a mechanism change. If the same data are plotted as a function of carbon, the mechanism change for the PTs becomes clear, see Fig. 2(d).

For carbon concentrations above 125 ppm in Zr–2.5Nb, only carbide particles greater than 1 μm are predominately present in CANDU® pressure tubes [12]. At concentrations below 125 ppm, particles less than 1 μm are present. The sharp distinction between the sizes has been documented and reported in Ref. [12] and is a result of the thermo-mechanical pressure tube treatment during fabrication. It is postulated that the perturbation in the pressure tube pickup curves as shown in Figs. 1(e) and 2(d) is likely due to the reduction of carbon from solid solution. As the number of large carbides increase, the pickup rate correspondingly increases, giving rise to the upswing at 125 ppm. Fig. 2(d) demonstrates that more work is required on microstructures and that a proper evaluation of the performance of pressure tubes must be carried out on material with PT microstructures. It is safe to say, however, regardless of any mechanistic changes, the lower the residual carbon concentration, the lower the deuterium pickup.

Each weight datum in Fig. 1 is derived from a different specimen and not from the batch average. The process of obtaining the deuterium pickup value (and indirectly, the oxygen value) destroys the specimen. The oxygen pickup data in Figs. 1(b), (d) and (f) are within 15–20% of the batch average total weight gain (deuterium plus oxygen), therefore, it is expected that deuterium data are representative of the average batch behaviour to within 15%.

Disparate trends in PTs and DCs pickup data are not surprising since there exist microstructural differences between the two types of materials and because each PT possessed a different impurity spectrum. The DCs were manufactured from a single stock material with yet another impurity spectrum. Further, the DCs were processed differently than the PTs in terms of their thermal/

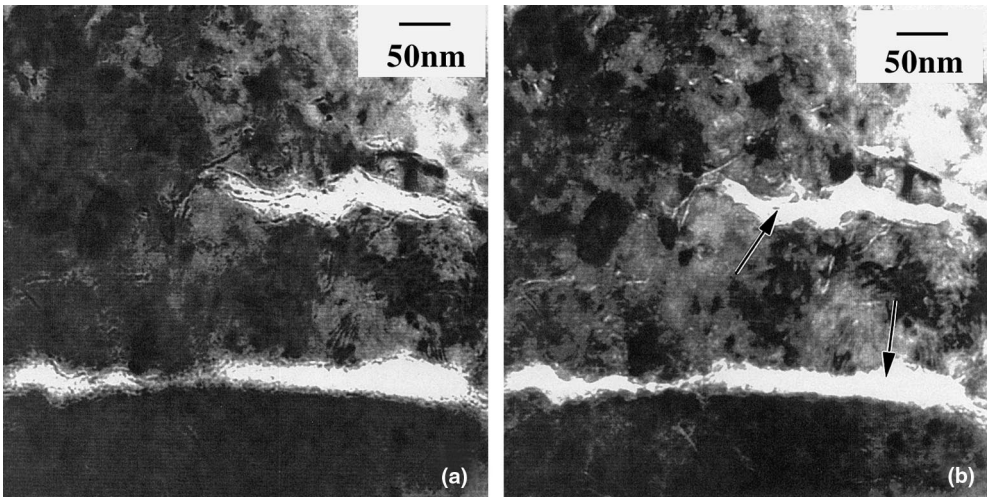

Fig. 3. Over- (a) and under-focus (b) of an oxide cross-section taken from the high-carbon material F5. Note the relatively large porosity marked by arrows.

mechanical histories. It may be surprising then that the data of Figs 1(a), (e) and (b), (f) are as similar as they are. The similarity likely indicates that residual carbon is far more effective in controlling deuterium pickup than say Fe or Si (see Table 1). Fig. 1 suggests that reducing residual carbon concentrations to less than 80 ppm would be beneficial.

For the drop-castings, the impurity analyses in Table 1 were performed after manufacture and are accurate to within 5%. The pressure tube specimens (F series in Table 1) were analyzed at seven points along the length of the Zr–2.5Nb ingot (before being sectioned and extruded into tubes) and averaged. The spread in impurity concentrations along the ingot is typically 15%. In a number of cases, impurity analyses were performed on off-cuts from the tube being tested but, again the actual concentrations are likely no more accurate than 5–10%.

3.2. Oxide microstructure

As illustrated in Fig. 1, there is an increasing amount of deuterium absorbed by the alloys over the range of carbon concentrations tested. Since deuterium must pass through the oxide before it enters the alloy, it is reasonable to expect that structural differences may exist in

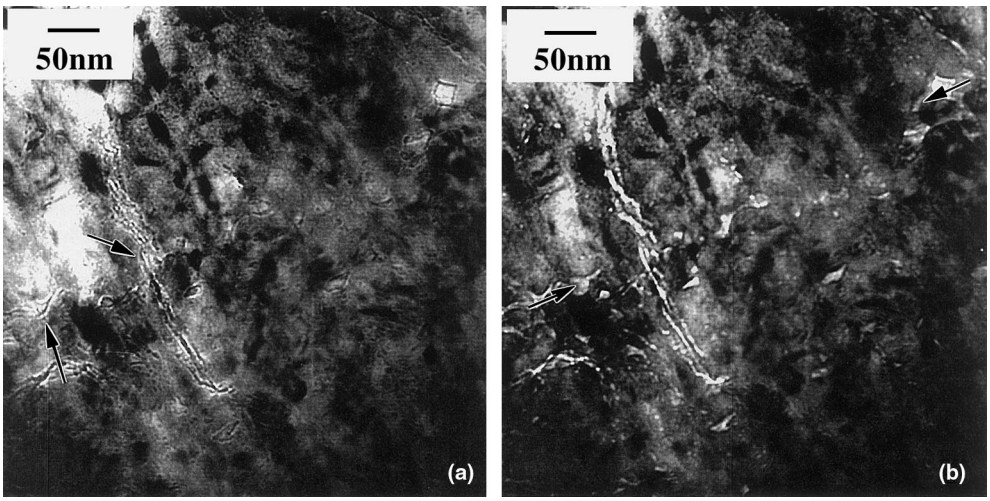

Fig. 4. As Fig. 3 but for the low-carbon material, F1. (a) Examples of the fine porosity, marked with arrows, common to oxides grown on low-carbon alloys. (b) An example, between the arrows, of fine pore alignment. Fine porosity of this type is difficult to detect except by Fresnel imaging.

the oxides of low- and high-carbon materials. Electron microscopy of oxide cross-sections revealed such suspected differences. Two were seen in the oxide films; the number density of a particular type of porosity and secondly, the oxide stoichiometry.

The likelihood of oxide porosity having developed in-situ, during the corrosion process, rather than as a result of specimen preparation for electron microscopy, was discussed in a separate publication [11]. One reason for oxide porosity not being more fully investigated in the past has been because of the need to defocus the electron microscope image, a procedure which does not come easily to a Microscopist who usually strives for the sharpest image possible. The evidence from electron microscopy for porosity can be easily missed without using the technique of Fresnel imaging. Small amounts of over- and under-focusing of the electron image creates, respectively, black and white fringes that circumscribe the pore boundaries making them easier to detect. Further, the presence of Fresnel fringes also indicates that the area being investigated is a pore. Fringes result when there is a large atomic potential difference between two neighbouring objects.

Figs. 3(a) and (b) are a Fresnel image pair showing an example of relatively large porosity which was commonly present in the oxide films grown on high-carbon material (batch *F*5, 145 ppm C). The porosity was often, but not always, associated with localized concentrations of Si, Fe or Al and often filled with a low density, amorphous material (most obvious in dark-field images). The coarse, as well as fine porosity, has been defined in another publication [11]. Coarse porosity was on average defined as 40–90 nm in length and 5–15 nm in width and fine porosity as 'wormholes' 5–30 nm in length and about 1 nm in width. Although dimensions were given in [11], further work has indicated that the thickness of the oxide foil must be kept in mind as the coarse porosity twists and turns throughout the bulk of the oxide (not just the foil thickness) so that any given oxide foil samples only a section of the porosity. The fine porosity is actually flake and not wormhole in character. Further details can be found in [13,14]. Dozens of specimens and oxide foils have been examined to reach the conclusions reported in [13,14].

Figs. 4(a) and (b) were images taken from the oxide grown on the low-carbon alloy (batch *F*1, 85 ppm C). These Fresnel images reveal a much finer type of porosity. Although this type of porosity was present in both the high- and low-carbon materials, it was more obvious in the oxide of the low-carbon material due to the relative deficiency of the coarse variety. Fine porosity was often found segregated in planes parallel to the free surface which is also co-linear with the predominant long direction of the β filament, in the plane of the image. In Fig. 4(b) a layer of fine porosity can be seen between the arrows.

The oxide crystallites in oxides grown on low-carbon alloys were more equi-axed than the columnar growths in oxides grown on high-carbon alloys but, because of the inhomogeneous manner in which all oxide films develop, this observation could be suspect without a great deal more investigation. Not only were the oxides grown on low-carbon alloys apparently more equi-axed but they were also suggestions that they might be less stoichiometric.

In oxide films formed on high-carbon material (material *D*5 in Table 1) and immediately below some of the large pores (on the o/m side of the pore), the oxide was sub-stoichiometric and composed of equi-axed crystallites [11]. A similar observation was noted for oxides formed on low-carbon material (*D*2 in Table 1) but sub-stoichiometric oxide formed near the oxide/metal interface and equi-axed crystallites were more common than columnar. If this observation holds with further investigation, it would suggest that fine porosity is not interconnected from the free surface to the oxide/metal interface. A large pore could result in the loss of cohesion with the underlying matrix and a local reduction in the oxygen partial pressure leading to sub-stoichiometry (i.e., in the competition for the available oxygen, oxygen-dissolution in the metal prevails). If the fine pores were interconnected then the oxygen partial pressure within the oxide would be sufficient to maintain stoichiometry. The low density material within the large pores may be dissolved zirconia stimulated by high pD water.

High residual carbon concentrations apparently result in horizontally and vertically connected porosity which permits oxygen and deuterium access to the oxide/metal interface. In oxides grown on low-carbon materials, which contain stratified fine porosity, the same degree of inner interface access is not present and this leads to non-stoichiometry and equi-axed oxide crystallite growth (oxygen is thermodynamically more stable in solid solution). The reason for the predominance of a specific type of porosity is the subject of two publications on oxide porosity [13,14]. Those publications indicate that any change in chemical impurity levels which affect the β-phase will also affect the deuterium pickup rate. If there is a change in the deuterium pickup curve around 110–120 ppm carbon, it is likely associated with changes in the β-phase, however, this is speculative and more work is required to test this hypothesis.

4. Conclusions

Corrosion tests in pressurized heavy-water at 575 K and pD 10.5, revealed a correlation between residual carbon concentrations in Zr–2.5Nb and the rate of deuterium absorption. A correlation also exists for oxide film formation, albeit to a lesser degree. Tests on Zr–2.5Nb–*x*C drop-castings indicated that after a few 100

days of corrosion, there is an almost linearly increasing variation in deuterium pickup with carbon concentration between 40 and 300 ppm carbon. Corrosion of CANDU® pressure tubes confirmed the correlation, but also suggested that, as seen earlier in the case of the drop-castings, there may be a perturbation in the deuterium pickup rate around 110–130 ppm of residual carbon.

Cross-sections of oxides grown on high- (145 ppm) and low-carbon (80 ppm) alloys revealed that the oxides from the high-carbon materials contained relatively large-sized porosity, whereas oxides from the low-carbon alloys were predominately composed of layered, fine porosity (parallel to the free surface). The oxide on low-carbon material also displayed a lower stoichiometry. It is likely that the deuterium pickup rate is controlled by oxide porosity.

Acknowledgements

Thanks are given to Wah Chang of Albany, Oregon (USA) who donated the Zr–2.5Nb–xC alloys. The contributions of A.E. Unger and M.S.G. Bergin, both of whom conducted the corrosion tests, are gratefully acknowledged. The Analytical Electron Microscopy reported in Section 3.2 was performed under contract by S.B. Newcomb and W.M. Stobbs (deceased) of SAM at the University of Cambridge, England.

References

[1] B. Cox, in: M.G. Fontana, R.W. Staehle (Eds.), Advances in Corrosion Science and Technology, Plenum, New York, 1970, p. 173.
[2] S. Kass, J.D. Grozier, National Assoc. Corrosion Engineers 20 (1961) 158t.
[3] G. Vigna, L. Lanzani, G. Domizzi, S.E. Bermúdez, J. Ovejero-García, R. Piotrkowski, J. Nucl. Mater. 218 (1994) 18.
[4] M.B. Elmoselhi, B.D. Warr, S. McIntyre, in: A.M. Garde, E.R. Bradley (Eds.), Zirconium in the Nuclear Industry, Tenth International Symposium, ASTM, Philadelphia, STP, 1993, p. 62.
[5] N. Ramasubramian, in: C.M. Eucken, A.M. Garde (Eds.), Zirconium in the Nuclear Industry, Ninth International Symposium, ASTM, Philadelphia, STP, 1991, p. 613.
[6] G.P. Sabol, S.G. McDonald, G.P. Airey, in: J.H. Schemel, H.S. Rosenbaum (Eds.), Zirconium in Nuclear Applications, ASTM, Philadelphia, STP, 551, 1973, p. 435.
[7] A.W. Urquhart, D.A. Vermilyea, in: J.H. Schemel (Ed.), Zirconium in Nuclear Applications, Rosenbaum, ASTM, Philadelphia, STP, 1973, p. 463.
[8] B. Cox, J. Nucl. Mater. 29 (1969) 50.
[9] B. Cox, Pore J. Nucl. Mater. 148 (1987) 332.
[10] B.D. Warr, P.A.W. Van der Heide, M.A. Maguire, in: E. Ross Bradley, George P. Sabol (Eds.), Zirconium in the Nuclear Industry: 11th International Symposium, ASTM, West Conshohocken, PA, STP, 1996, p. 265.
[11] R.A. Ploc, in: S.B. Newcomb, J.A. Little (Eds.), Proceedings of the Third International Conference, 16–18 September 1966, University of Cambridge, The Institute of Materials, London, 1997, p. 475.
[12] J.R. Theaker, R. Choubey, G.D. Moan, S.A. Aldridge, L. Davis, R.A. Graham, C.E. Coleman, in: A.M. Garde, E.R. Bradley (Eds.), Zirconium in the Nuclear Industry, Tenth International Symposium, ASTM, Philadelphia, STP, 1993, p. 221.
[13] R.A. Ploc, in: Proceedings of the Fourth International Conference on Microscopy of Oxidation, presented 20–21 September 1999, University of Cambridge, to be published.
[14] R.A. Ploc, G.A. McRae, in: Proceedings of the 14th International Corrosion Congress, 27 September–1 October 1999, Cape Town, South Africa, to be published.